JOURNAL OF APPLIED ELECTROCHEMISTRY 21 (1991) 508–515

In situ activation of cathodes during alkaline water electrolysis by dissolved iron and molybdenum species

L. BROSSARD, J.-Y. HUOT*

Institut de Recherche d'Hydro-Québec (IREQ), 1800 Montée Ste-Julie, Varennes, Québec J3X 1S1, Canada

Received 8 June 1990; revised 4 September 1990

In situ activation on polished pure Co, Fe, Ni and Pt cathodes by the dissolution of molybdenum in 30 wt % KOH at 70° C was investigated at $100\,\text{mA}\,\text{cm}^{-2}$. The effect of adding molybdate to the electrolyte to reactivate hydrogen discharge depends on the concentration of dissolved iron. The deposition of Mo on the substrate takes place only in the presence of this metallic impurity. The best improvement of the hydrogen evolution reaction is reported when iron alone is dissolved in the electrolyte. The nature of the changes occurring on the cathode surfaces during hydrogen evolution was demonstrated by scanning electron microscopy and X-ray microanalysis.

1. Introduction

Long operating periods in industrial water electrolysis call for hydrogen and oxygen overpotentials, stable performance and available *in situ* activation techniques.

For the hydrogen evolution reaction (HER), *in situ* activation was first described by Jaksić and Csonka [1] in the case of the electroreduction of molybdate in alkaline solutions. The phenomena was ascribed to the direct reduction in molybdenum oxide and the further indirect reduction by hydrogen in active metallic molybdenum. It was shown that *in situ* codeposition of Mo and Co [2] or *ex situ* codeposition of Mo and Fe [3] promotes the electroreduction of molybdate, while an electrocatalytic effect was attributed to synergetic Mo–Co codeposit [2] and Mo–Fe coating [4]. This synergy is in agreement with synergetic electrocatalysts identified from Brewer's theory [5].

Time effects on nickel [6–8], cobalt [9], platinum [10] and other metallic [11] electrodes have been reported in 30 wt % KOH containing metallic impurities such as iron (0.5 ppm). At high cathodic current density, or overpotential, the deactivation process during the first hours of polarization is ascribed to hydrogen absorption, while for longer times the formation of iron-base metallic deposits influences the hydrogen discharge.

The addition of several ppm of sodium molybdate [7–9, 12] or iron [10] to the unpurified electrolyte significantly reduces the deactivation rate owing to hydrogen absorption and KOH metallic impurities and improves the electrocatalytic activity for the HER. In the case of iron activation, the effect was attributed to a porous deposit of pure iron [10], whereas molybdate activation was attributed to codeposition of molybdenum and KOH metallic impurities [8, 12]. The resulting *in situ* activation process is fast [7, 11] and a porous metallic deposit can be observed in the electrode substrate within 10^4 s of polarization.

The present investigation focuses on the *in situ* activation of pure Co, Fe, Ni and Pt cathodes in unpurified 30 wt % KOH at 70° C in the presence of 0.25 mM (14 ppm) dissolved iron or 0.25 mM iron plus 0.25 mM sodium molybdate. The alkaline water electrolysis was performed at $100\,\text{mA}\,\text{cm}^{-2}$.

2. Experimental details

The electrochemical meaasurements were carried out in 30 wt % KOH aqueous solutions at 70° C. The cell is described in detail elsewhere [2, 3]. The working electrode consisted of vertical Co, Fe, Ni or Pt wires (99.99%), 0.05 cm in diameter, which gave a sample surface area of $0.31\,\text{cm}^2$. The samples were not exposed to heat treatment prior to the experiments; they were polished with $\approx 0.3\,\mu\text{m}$ of alumina paste.

The temperature was maintained constant at 70° C by means of a Lauda M20 thermostatic bath. Polarization curves were obtained by galvanostatically lowering the applied current from $100\,\text{mA}\,\text{cm}^{-2}$, where it was kept for a given period of time, to $10\,\text{mA}\,\text{cm}^{-2}$. The cathode potential was recorded against time at $100\,\text{mA}\,\text{cm}^{-2}$. Impedances were measured with a Solartron 1250 frequency response analyser.

The reversible potential for the HER was measured by bubbling hydrogen against a platinized platinum electrode immersed in 30 wt % KOH solution at 70° C. The value was -0.962 V with respect to the Hg/HgO/KOH 1 M reference electrode at 70° C.

Some of the 30 wt % KOH solutions were enriched with 14 ppm (0.25 mM) of Fe (II) and/or Fe (III) species by anodically dissolving an iron electrode in 30 wt % KOH at 70° C at a potential of $-0.9\,\text{V}_{\text{Hg/HgO}}$

---

* Present address: Centre de Technologie Noranda, 240 boulevard Hymus, Pointe-Claire, Québec, Canada, H9R 1G5.

according to the procedure described by Armstrong and Baurhoo [13]. Eventually, 0.25 mM of sodium molybdate was dissolved in this electrolyte.

Alternatively, fresh 30 wt % KOH solutions were pre-electrolyzed for ≈48 h to remove the electrolyte impurities. A nickel cathode with a geometric surface area of ≈ 100 cm^2 was used with a 100 cm^2 nickel anode, while the applied current was 100 mA (1 mA cm^{-2}).

From impedance measurements and fitting of the *i–E* data and taking into account the resistive factor, the ohmic resistance at 100 mA cm^{-2} was evaluated as being typically 0.4 Ω cm^{-2}.

3. Results and discussion

3.1. *In the presence of 0.25 mM dissolved iron*

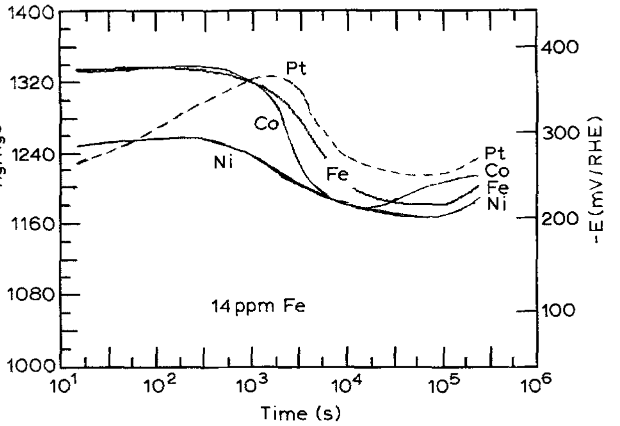

Fig. 1. Cathode potential behaviour against time under galvanostatic control at 100 mA cm^{-2} in the presence of 14 ppm (0.25 mM) dissolved iron in 30 wt % KOH at 70° C.

Typical potential against time curves for an applied cathodic current density of 100 mA cm^{-2} are illustrated in Fig. 1 for Co, Fe, Ni and Pt cathodes. The shape of the *E–t* curves is similar for the Co, Fe and Ni cathodes. All four electrodes undergo activation ranging from 100 to 150 mV between 10^3 and 10^4 s. The main differences between some of the electrodes are the initial activity, as displayed by the initial potential value and the time to reach minimum potential after activation. Deactivation at a rate of 70 mV dec^{-1} occurs after 1.8 × 10^4 s for Co and after 10^5 s for the three other substrates (Fig. 1). This phenomenon indicates the absence of a steady state for the *in situ* activated electrodes and the difficulty of reducing the experimental hydrogen overpotential at 100 mA cm^{-2} below 160 mV.

The morphology and nature of the cathode surfaces were investigated by scanning electron microscopy (SEM) and X-ray microanalysis (EDX) to determine whether KOH metallic impurities and additives are deposited during the hydrogen evolution. The samples were examined after a polarization time ranging from 0 to 2.4 × 10^5 s at 100 mA cm^{-2}. Since the four electrodes display equivalent morphologies, only the case of cobalt is illustrated (Fig. 2). The initial surface is smooth and free of metallic deposit but, after 10^3 s, a slight roughness is observed (Fig. 2a) owing to the deposition of iron on the substrate. The iron deposit increases significantly with the polarization time and the morphology of the cathode surface also changes from 10^3 to 2.4 × 10^5 s. All the substrates became covered with pure iron. The cyclic voltammogram of platinum showed the same characteristics as the voltammogram of a pure iron electrode but with more intense anodic peaks, which are attributed to the roughness of the iron coating [10]. At 10^4 s very small crystallites of iron are mixed with larger ones about 3 μm long (Fig. 2b). The size of these crystallites increases with polarization time but after 7.5 × 10^4 s, many form needles which display deposition planes at 2.4 × 10^5 s (Fig. 2c, d).

The values of the exchange-current density, i_0, and the Tafel slope, b, for the HER at various times, during which the applied-current density was maintained constant at 100 mA cm^{-2}, are summarized in Table 1 for the four cathodes. For all substrates, i_0 and b increase considerably with polarization time from 10^4 to 24 × 10^4 s and reach much the same values, but the overall time effect on the calculated overpotential at 100 mA cm^{-2} remains slight.

Impedance measurements were performed from 0.1 Hz to 4 kHz, after 7.5 × 10^4 s at 100 mA cm^{-2}. For all four cathodes, the impedance diagram resulted in a semicircle (Fig. 3) from which the ohmic resistance, charge transfer resistance and double-layer capacitance were calculated. The charge transfer resistance ranged from 0.7 to 0.8 Ω cm^2 while the double-layer capacitance (C_{dl}) reached values of 1300 μF cm^{-2} (Table 2). This high C_{dl} value is ascribed to the deposit of iron crystallites on the cathode surface, which is in agree-

Table 1. Kinetic parameters of the HER at different polarization times at 100 mA cm^{-2} in 30 wt % KOH, containing 14 ppm of iron, at 70° C

Substrate	*Polarization time*					
	10 000 s		*75 000 s*		*240 000 s*	
	b *(mV)*	i_0 *(mA cm^{-2})*	b *(mV)*	i_0 *(mA cm^{-2})*	b *(mV)*	i_0 *(mA cm^{-2})*
Co	36	0.96 × 10^{-3}	79	0.13	101	0.35
Fe	39	0.47 × 10^{-3}	80	0.14	79	0.16
Ni	89	0.72 × 10^{-1}	95	0.21	109	0.73
Pt	51	6.6 × 10^{-3}	75	0.06	104	0.34

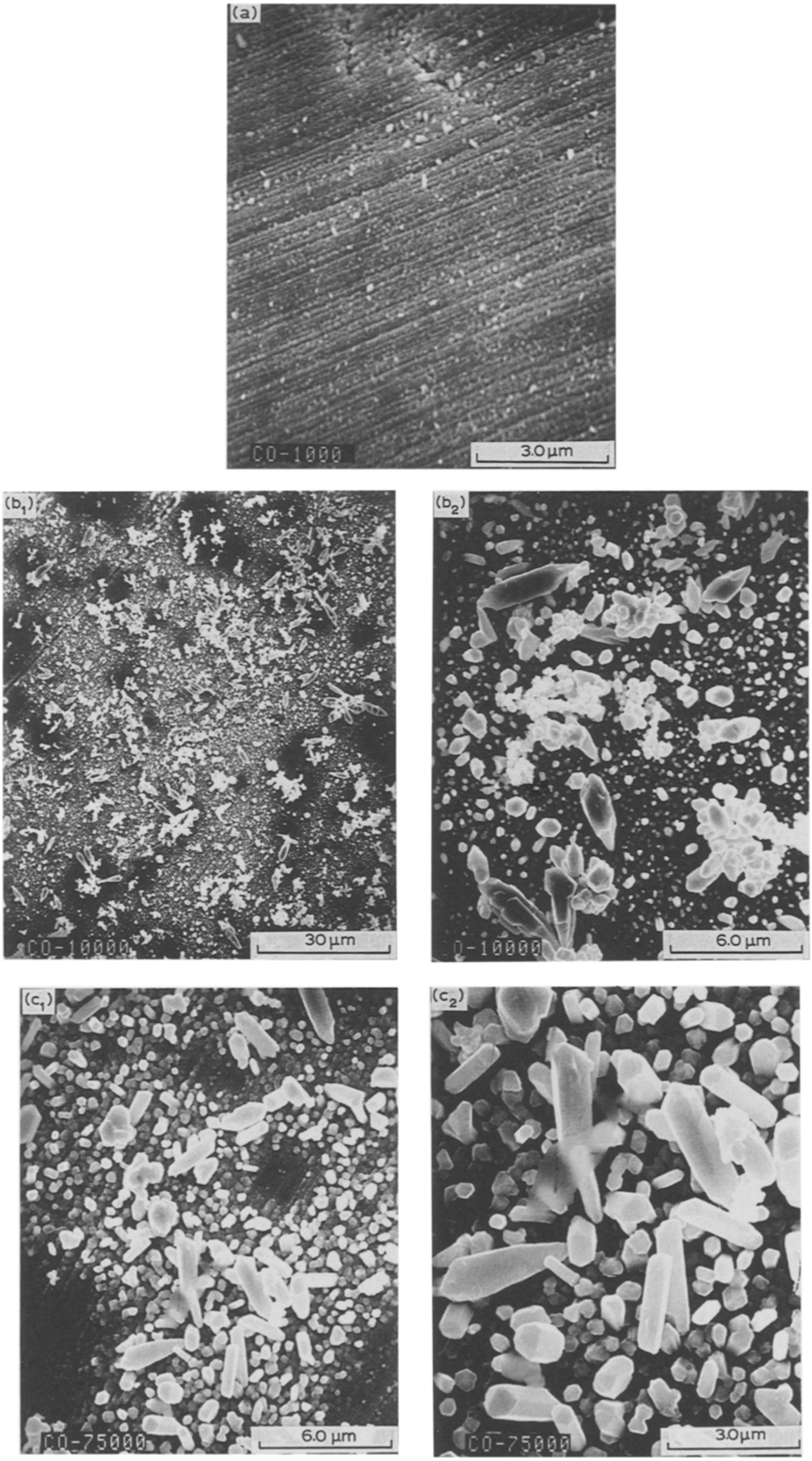

Fig. 2. Cobalt cathode surface during HER at constant applied current of 100 mA cm^{-2} in 30 wt % KOH (0.25 mM Fe) at 70° C. Times of removal are: (a) 1000 s, (b) 10 000 s, (c) 75 000 s, (d) 240 000 s. The corresponding composition of the cathode surface by EDX analysis are (at %): (a) Fe 10%, Co 90%, (b) Fe 39%, Co 61%, (c) Fe 53%, Co 47%, (d) Fe 78%, Co 22%.

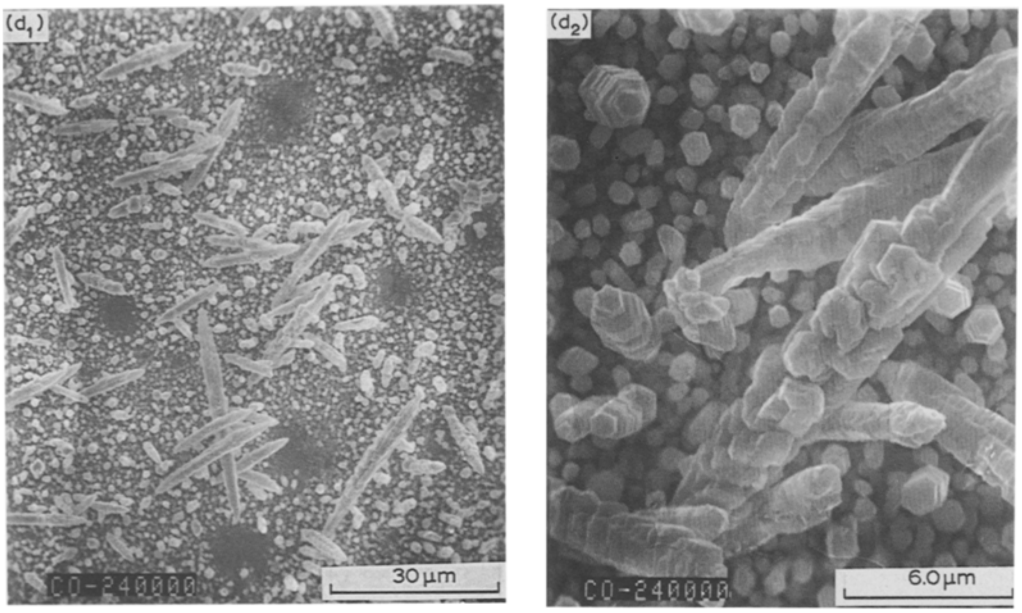

Fig. 2. Continued.

ment with the formation of a similar iron deposit on the four substrates. In fact, the electrocatalytic activity is practically the same for the four substrates after 75 000 s of polarization at 100 mA cm^{-2}, as illustrated by experimental overpotentials given in Table 2. The surface morphology of the iron deposit is also similar for all substrates. These characteristics are in agreement with the similar electrode-solution interface properties observed for the four substrates under the same experimental conditions.

Concerning the formation of crystallites, a recent investigation into amorphous alloy containing iron [14] showed the improved electrode activity to be associated with the formation of very fine particles rich in iron on the amorphous matrix resulting in a significant reduction of the hydrogen overvoltage. For the amorphous alloy containing iron, the size of the iron crystallites is in the order of 0.1 μm compared to 1 μm in the present case. This is in agreement with the fact that i_0 and C_{dl} are approximately ten times higher in the case of amorphous alloys, while the Tafel slope is approximately the same in the case of pure iron coating (Tables 1, 2, and [14]).

3.2. *In the presence of 0.25 mM dissolved molybdenum*

It is generally accepted that molybdenum can be deposited in aqueous solutions only when another metallic species is present in the electrolyte and can be codeposited with the molybdenum [3, 15]. It is not surprising that the potential against time relationships are practically the same in the presence (Fig. 4) or absence [7, 9, 10] of dissolved molybdenum, since the starting solution is pre-purified in both cases.

For example, the deactivation rate (*i.e.* the slope

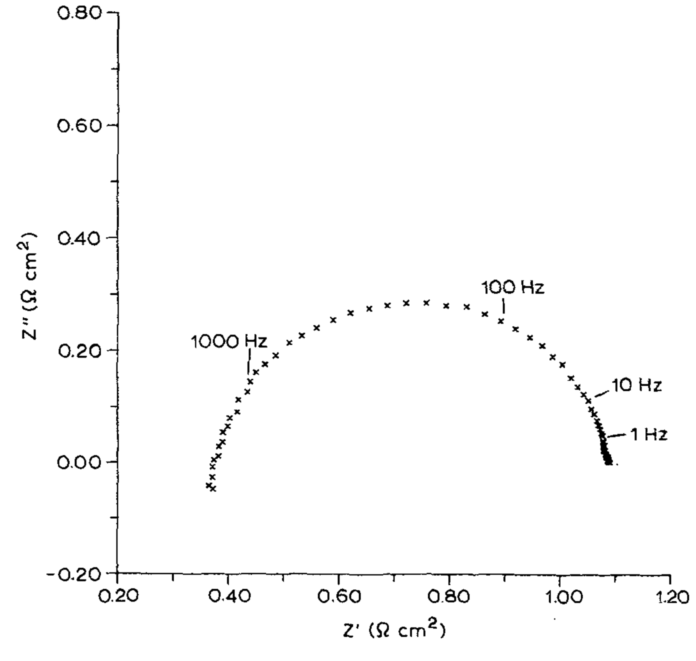

Fig. 3. Experimental impedance spectra for the Ni cathode at 100 mA cm^{-2} after 75 000 s polarization at this current density.

Table 2. Results of the impedance measurements taken after 75 000 s at 100 mA cm^{-2} in 30 wt % KOH, containing 14 ppm of iron, at 70° C

Substrate	R_{ct} ($\Omega\,cm^2$)	C_{dl} ($\mu F\,cm^{-2}$)	ϕ* (*deg*)	η_{100} (*mV*)
Co	0.69	1220	11	228
Fe	0.73	1330	14	226
Ni	0.71	1360	12	254
Pt	0.83	1330	19	242

* ϕ depression angle.

dE/d log t) of the Pt cathode is 124 mV decade^{-1} time between 10^2 s and 10^3 s in a purified electrolyte containing dissolved molybdenum compared to 100 mV decade^{-1} time in the absence of molybdenum [10]. The variation of potential with time is negligible for the cobalt cathode from 10 to 75 000 s in the presence of 0.25 mM dissolved molybdate. The hydrogen overpotential is approximately the same for the Fe, Ni and Pt cathodes after 75 000 s of polarization at 100 mA cm^{-2} with 0.25 mM Mo.

It is deduced from the SEM and EDX analyses of the cathode surface that the substrates remain free of deposited metallic species such as molybdenum for up to 75 000 s under a cathodic current of 100 mA cm^{-2} in the presence of 0.25 mM dissolved molybdenum. This observation supports the mechanism of codeposition of Mo with KOH metallic impurities [7–9, 11, 12] in strongly alkaline solutions.

3.3. *In the presence of 0.25 mM Fe + 0.25 mM Mo*

Potential versus time curves for an applied cathodic-current density of 100 mA cm^{-2} are shown in Fig. 5 for the four substrates under investigation in 30 wt % KOH, containing 0.25 mM dissolved Fe plus 0.25 mM dissolved Mo, at 70° C. In all cases, deactivation of the cathode is observed immediately after polarization starts; the deactivation rate and duration depend on the nature of the substrate. An equivalent activation occurs after 500 s for all substrates. In the case of Pt, deactivation is evident for the first 500 s of polarization and its rate is 67 mV decade^{-1}. In the case of Fe, the deactivation rate is only 2.5 mV decade^{-1} and the deactivation time is 100 s. For times exceeding the deactivation time, the Pt cathode undergoes activation at a rate of 20 mV decade^{-1} compared to the 27 mV decade^{-1} observed for Co and Fe.

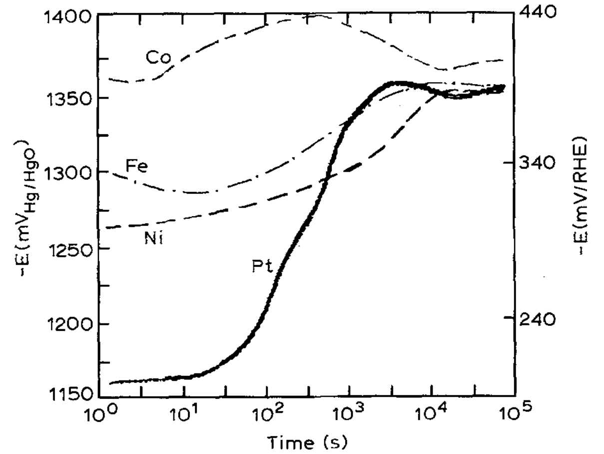

Fig. 4. Cathode potential behaviour against time under galvanostatic control at 100 mA cm^{-2} in the presence of 0.25 mM Mo. The electrolyte, 30 wt % KOH at 70° C, was previously electrolyzed to remove dissolved iron contained as an impurity in KOH.

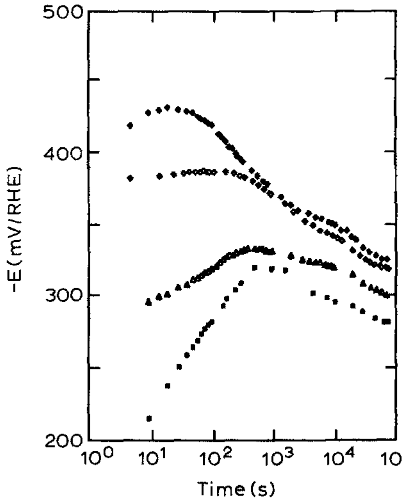

Fig. 5. Cathode potential behaviour against time under galvanostatic control at 100 mA cm^{-2} in the presence of 0.25 mM Mo + 0.25 mM Fe (30 wt % KOH, 70° C) (◆) Co, (◇) Fe, (△) Ni and (■) Pt.

Figure 6 shows the cathode surfaces after 75 000 s of polarization at 100 mA cm^{-2} in the presence of 0.25 mM Fe + 0.25 mM Mo. The morphology and composition of the deposit are practically independent of the nature of the substrate but the addition of Mo results in small changes in the morphology of the iron coating (Figs. 2c, 6a, 6b). The corresponding Tafel parameters for the HER are summarized in Table 3. The addition of molybdenum to the electrolyte containing dissolved iron results in a large increase of the Tafel slope and exchange-current density (Tables 1 and 3), the hydrogen overvoltage being significantly higher with dissolved molybdenum (Figs. 1 and 5), for example, 80 mV higher in the case of the Ni substrate after 75 000 s at 100 mA cm^{-2}. This behaviour is related to the HER being different in the presence and absence of Mo, although the exact nature of this difference is not clearly understood.

The morphology and composition of the metallic coating are quite different when the nickel cathode is

Table 3. Tafel parameters for the HER on different substrates after 75 000 s at 100 mA cm^{-2} in the presence of 0.25 mM Mo + 0.25 mM Fe

Substrate	*b* (*mV*)	i_0 (*mA cm*$^{-2}$)
Co	151	0.45
Fe	154	0.81
Ni	182	1.50
Pt	163	0.72

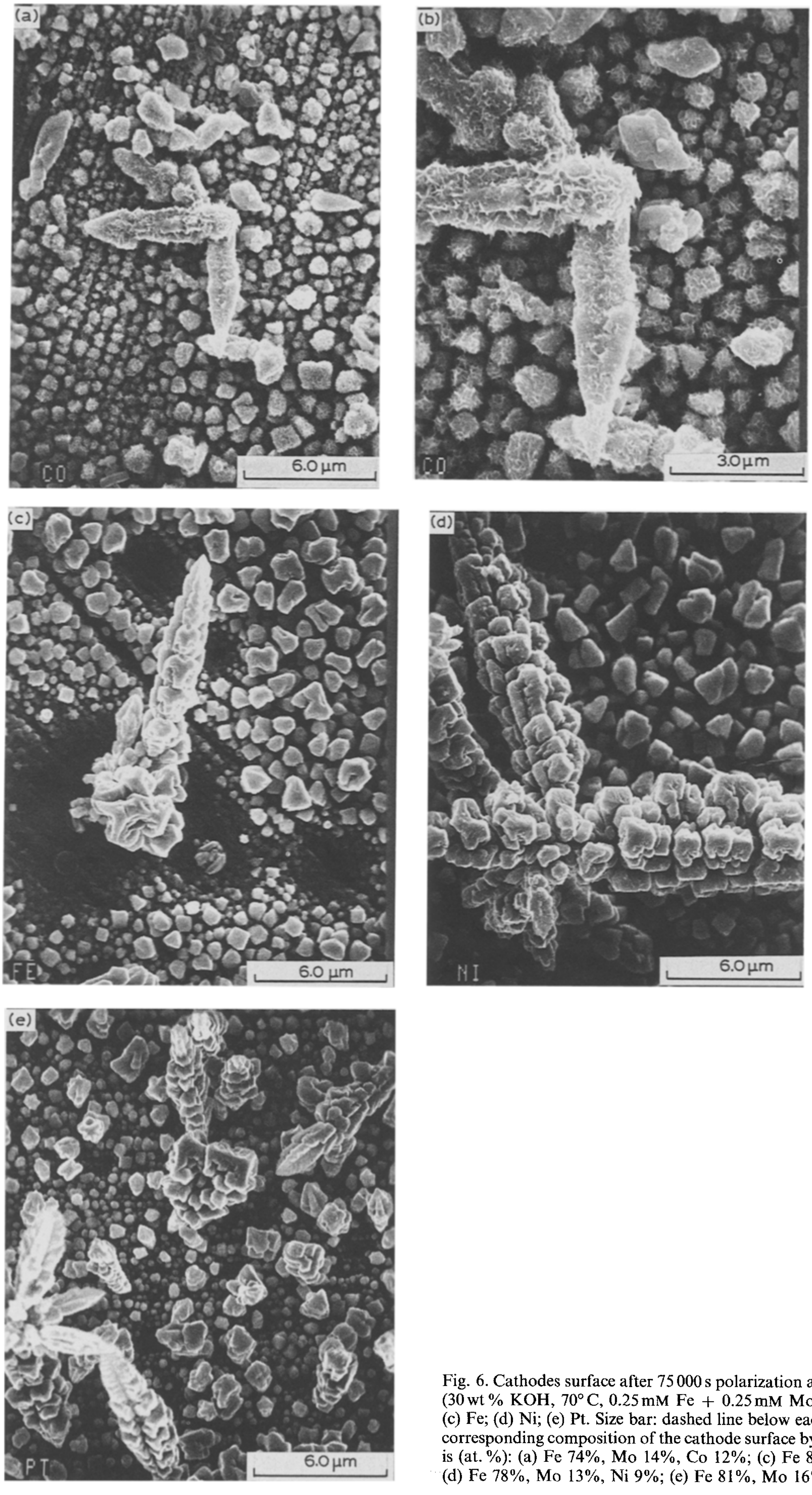

Fig. 6. Cathodes surface after 75 000 s polarization at 100 mA cm^{-2} (30 wt % KOH, 70° C, 0.25 mM Fe + 0.25 mM Mo). (a + b) Co; (c) Fe; (d) Ni; (e) Pt. Size bar: dashed line below each picture. The corresponding composition of the cathode surface by EDX analysis is (at. %): (a) Fe 74%, Mo 14%, Co 12%; (c) Fe 88%, Mo 12%; (d) Fe 78%, Mo 13%, Ni 9%; (e) Fe 81%, Mo 16%, Pt 3%.

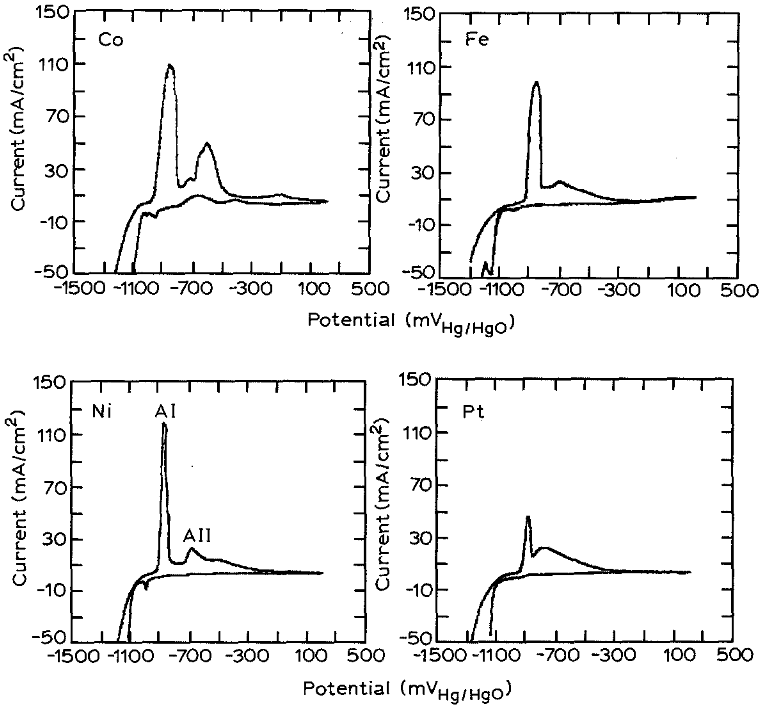

Fig. 7. Anodic portion of the single-cycle voltammograms in 30 wt % KOH at 70° C after cathodic polarization at 100 mA cm^{-2} in the presence of 0.25 mM Mo + 0.25 mM Fe. Sweep rate: 50 mV s^{-1}.

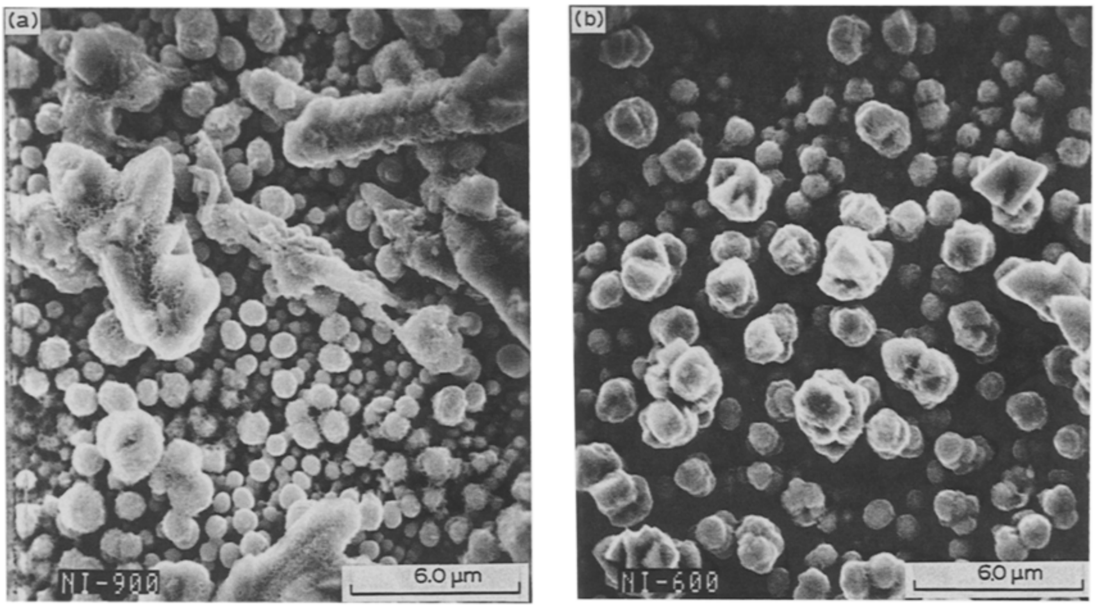

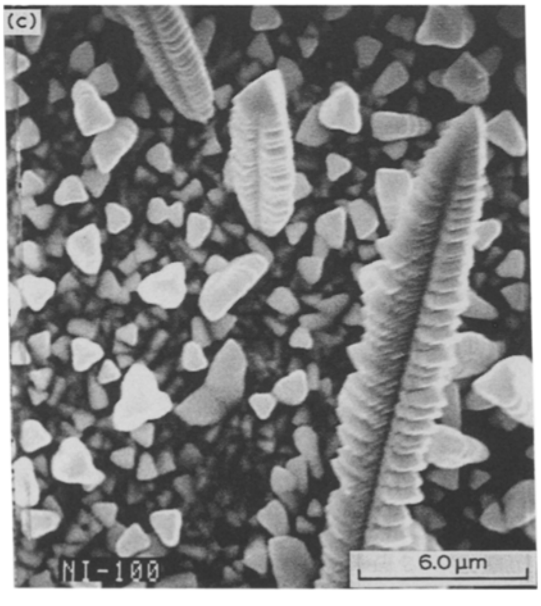

Fig. 8. Nickel cathodes after 75 000 s polarization at 100 mA cm^{-2} and potential sweep in the anodic direction at 50 mV s^{-1} (0.25 mM Mo + 0.25 mM Fe). Potential at which the cathode was removed: (a) $-950\,mV_{Hg/HgO}$; (b) $-800\,mV_{Hg/HgO}$; (c) $-150\,mV_{Hg/HgO}$. Size bar: dashed line below each picture. The corresponding composition of the cathode surface by EDX analysis (at. %): (a) Fe 78%, Mo 13%, Ni 9%; (b) Fe 84%, Mo 9%, Ni 7%; (c) Fe 87%, Mo 7%, Ni 6%.

polarized in the presence of 0.5 ppm Fe + 4 mM Mo [12]. After 10^5 s of polarization, the metallic deposit is spongy and contains more molybdenum than iron. The corresponding values of b and i_0 are 152 mV and 0.45 mA cm^{-2}, respectively, and the hydrogen overpotential at 100 mA cm^{-2} (η_{100}) is 357 mV. In the case of the Ni substrate polarized for 75 000 s (Table 3), larger values of b and i_0 are observed; η_{100} is 332 mV. It should be mentioned that the calculated η_{100} is very sensitive to the presence of deposited molybdenum: it increases by more than 100 mV as Mo becomes a major component in the deposit. In addition, the nickel content observed by EDX analysis is much larger in the presence of 0.5 ppm Fe + 4 mM Mo (Table 2 and [12]), which tentatively suggests that the amount of deposited material is different in both cases. The latter variable may also influence the electrocatalytic activity of the metallic coatings.

The hydrogen overpotential of the Ni cathode at 100 mA cm^{-2} after 75 000 s of polarization is $\sim$332 mV in the presence of 0.25 mM Fe + 0.25 mM Mo compared to $\sim$372 mV in the presence of 9×10^{-3} mM Fe + 0.25 mM Mo [12]. The improved electrocatalytic activity of the deposit formed in the presence of 0.25 mM Fe + 0.25 mM Mo is attributed to the formation of crystallites of metallic iron on a Ni substrate (Fig. 6d). It is reported that Fe–Mo coating obtained by thermal decomposition of various composite salt mixture at elevated temperatures on Ni substrate may be considered a synergetic electrocatalyst [4] according to the Brewer theory [5]. In the present investigation, it is deduced that the electrocatalytic activity for the HER may be related to the size of the iron-rich crystallites on the surface.

The anodic portions of single-cycle voltammograms for the Co, Ni and Pt cathodes are illustrated in Fig. 7. A constant-current density of 100 mA cm^{-2} (cathodic) was applied for 75 000 s in the presence of 0.25 mM Fe + 0.25 mM Mo. The electrodes were then potentiodynamically swept from the potential reached after 75 000 s at 100 mA cm^{-2} up to $+0.1\ \mathrm{V_{Hg/HgO}}$ and back at a scan rate of 50 mV s^{-1}, and the cell current was recorded.

Two oxidation peaks are dominant on those voltammograms. In the case of the Ni substrate, the first peak (AI) is located at $\sim -0.88\ \mathrm{V_{Hg/HgO}}$ and the second one (AII) at $\sim -0.69\ \mathrm{V_{Hg/HgO}}$. EDX analysis (Fig. 8) suggests that peak AI most likely corresponds to the partial oxidation of molybdenum accumulated in the deposit, which is in good agreement with the literature [8].

4. Conclusion

The loss of efficiency for the cathodic HER takes the form of increases in the cathodic overpotential at constant-current density. The addition of Mo to the 30 wt % KOH solution at 70° C has practically no influence on the time effect associated with the hydrogen discharge when the electrolyte is free from dissolved iron. The best improvement in the electrocatalytic activity is reported in the presence of dissolved iron only; the addition of Mo to those solutions has a detrimental effect on the HER.

References

[1] M. M. Jaksić and I. M. Csonka, *Electrochem. Technol.* **4** (1966) 49.

[2] C. M. Lacnjevac and M. M. Jaksić, *R. Res. Inst. Catal. Hokkaido Univ.* **31** (1983) 7.

[3] H. Fukushima, T. Akiyama, S. Akagi and K. Higashi, *Trans. Japan Inst. Metal* **20** (1978) 358.

[4] M. M. Jaksić, T. Grozdic and B. Kosanović, Brewer Intermetallic Phases as Synergetic Electrocatalysts for Hydrogen Evolution. Paper presented at Fall Meeting of the Electrochemical Society, Honolulu, Hawaii (1987).

[5] M. M. Jaksić, *Int. J. Hydrogen Energy* **12** (1987) 727; *Mat. Chem. and Phys.* **221** (1989) 1.

[6] H. E. G. Rommal and P. J. Moran, *J. Electrochem. Soc.* **132** (1985) 325.

[7] J.-Y. Huot and L. Brossard, *Int. J. Hydrogen Energy* **12** (1987) 821.

[8] *Idem, Surf. and Coatings Techn.* **34** (1988) 373.

[9] *Idem, J. Applied Electrochem.* **18** (1988) 815.

[10] *Idem, ibid.* **19** (1989) 882.

[11] *Idem, Int. J. Hydrogen Energy* **4** (1989) 229.

[12] *Idem, J. Applied Electrochem.* **20** (1990) 281.

[13] R. D. Armstrong and I. Baurhoo, *J. Electroanal. Chem.* **40** (1972) 325.

[14] J.-Y. Huot, M. Trudeau, L. Brossard and R. Schulz, *J. Electrochem. Soc.* **136** (1989) 2224.

[15] A. Brenner, 'Electrodeposition of Alloys', Vol. 2, Academic Press, New York (1963) chap. 34.